

Fuad A. Al-Horani · Tim Ferdelman  
Salim M. Al-Moghrabi · Dirk de Beer

## Spatial distribution of calcification and photosynthesis in the scleractinian coral *Galaxea fascicularis*

Received: 20 August 2003 / Accepted: 12 October 2004 / Published online: 8 December 2004  
© Springer-Verlag 2004

**Abstract** The spatial heterogeneity of photosynthesis and calcification of single polyps of the coral *Galaxea fascicularis* was investigated. Photosynthesis was investigated with oxygen microsensors. The highest rates of gross photosynthesis (Pg) were found on the tissue covering the septa, the tentacles, and the tissues surrounding the mouth opening of the polyp. Lower rates were found on the tissues of the wall and the coenosarc. Calcification was investigated by radioactive tracers. The incorporation pattern of  $^{45}\text{Ca}$  and  $^{14}\text{C}$  in the corallites was imaged with use of a Micro-Imager. The  $\beta$ -images obtained showed that the incorporation of the radioactive tracers coincided with the Pg distribution pattern with the highest incorporation rates found in the corallite septa. Thus, the high growth rate of the septa is supported by the high rates of Pg by the symbiont in the adjacent tissues. The total incorporation rates were higher in light than in dark, however, the distribution pattern of the radioisotope incorporation was not affected by illumination. This further emphasizes the close relation between calcification and photosynthesis.

**Keywords** Coral · *Galaxea fascicularis* · Calcification · Photosynthesis ·  $^{45}\text{Ca}$  ·  $^{14}\text{C}$  · Microsensors · Micro-Imager

Communicated by Biological Editor R.C. Carpenter

F. A. Al-Horani · T. Ferdelman · D. de Beer  
Max Planck Institute for Marine Microbiology,  
Celsiusstrasse 1, 28359 Bremen, Germany

*Present address:* F. A. Al-Horani (✉)  
Marine Science Station, P. O. Box (195),  
Aqaba, 77110, Jordan  
E-mail: f.horani@ju.edu.jo  
Tel.: +962-3-2015145  
Fax: +962-3-2013674

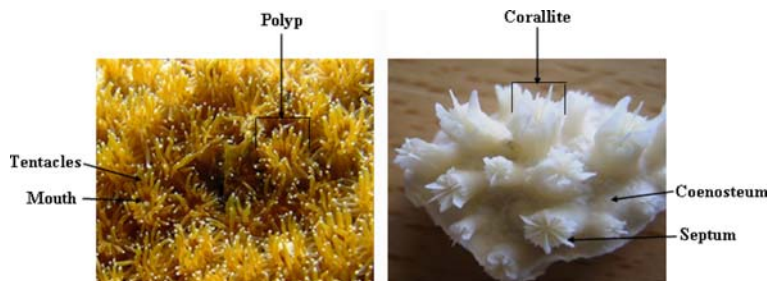
S. M. Al-Moghrabi  
Environmental Planning Directorate,  
P. O. Box (2565), Aqaba, 77110, Jordan

### Introduction

Scleractinian corals are  $\text{CaCO}_3$  skeletons covered by a thin layer of tissue. The colonies they form are made up of smaller building blocks, the polyps. The thin layer of tissue is composed of two epithelia separated by the body cavity, the coelenteron. The  $\text{CaCO}_3$  skeleton underneath the tissue layer is secreted by the animal and its shape is characteristic at the species level (Fig. 1). The corals have a symbiotic relationship with *Symbiodinium* sp. embedded in its endodermal cells. It has been long known that the rate of coral calcification is higher in light than in dark (e.g. Goreau 1959; Pearse and Muscatine 1971; Chalker and Taylor 1975). This light enhancement of calcification was attributed to photosynthesis by the symbiont, though the exact mechanism of this enhancement is not very well established (see reviews by Barnes and Chalker 1990; Allemand et al. 1998; Gattuso et al. 1999).

The overall coral shape is determined by the differential growth rates of its building blocks. Goreau (1959) noticed variation in the growth rates of the different parts of the coral colony. Furthermore, Marshall and Wright (1998) found that different parts of the polyp incorporate  $^{45}\text{Ca}$  and  $^{14}\text{C}$  differently. Similarly, it has been shown with microsensors that photosynthesis and calcium dynamics are heterogeneous on the coral surface (Kühl et al. 1995; De Beer et al. 2000). Yet, a study of the interactions between the symbiont photosynthesis and the animal calcification at a microscale level is still lacking. We have combined oxygen microsensors and Micro-Imager (both with ca. 10  $\mu\text{m}$  spatial resolution) to study the rates of photosynthesis and calcification on the different parts of the coral *Galaxea fascicularis* polyps. With this study we try to relate the heterogeneous polyp surface with its physiology. The effect of light, dark and isotopic exchange on the incorporation of  $^{45}\text{Ca}$ ,  $^{14}\text{C}$ -labelled bicarbonate and glucose were also studied.

**Fig. 1** Digital photographs of a *G. fascicularis* colony showing the heterogeneous polyps (left) and corallites (right)



## Materials and methods

### Biological samples

*G. fascicularis* colonies originated from the Gulf of Aqaba-Jordan were transferred to the Max Planck Institute, Bremen-Germany. They were maintained in an aquarium (35‰ salinity, pH around 8.2, light intensity of 140–170  $\mu\text{mol photons m}^{-2} \text{s}^{-1}$ , temperature of 26°C). Single polyps were fixed on small glass vials with underwater epoxy and left in the aquarium until a microcolony was developed and used in the incubation experiments.

### Measurement of photosynthesis

Clark type  $\text{O}_2$  electrodes (Revsbech and Jorgensen 1983) were used to measure gross photosynthesis (Pg) using the light/dark shifts as described previously (Kühl et al. 1995). The coral colonies were placed in a polycarbonate flow cell for microsensor measurements. Filtered seawater was circulated between the flow cell and a 3 l reservoir at a constant flow rate ( $450 \text{ ml min}^{-1}$ ). The reservoir was continuously aerated. Motorized micromanipulators fixed on a heavy stand were used to position the electrodes on different parts of the polyps. The electrodes were positioned immediately above the surface of the polyp tissue. A halogen light source (KL 1500 Schott Mainz company-Germany) provided a light intensity of  $170\text{-}\mu\text{mole photons m}^{-2} \text{s}^{-1}$ .

### Incubation with radioactive tracers

Coral colonies were incubated in a beaker containing 400 ml of filtered artificial seawater prepared from tropical marine salt (35‰ salinity pH of 8.2). The water was stirred and the temperature was maintained at 26°C. The incubation period was 5 h in all the experiments. Prior to addition of the radiotracer, the coral pieces were left for at least 1 h to recover from the transfer and acclimatize in the incubation conditions. Radioactive tracers, Ca as  $\text{CaCl}_2$ ,  $^{14}\text{C}$ -glucose, and  $^{14}\text{C}\text{-HCO}_3^-$  (Amersham Pharmacia Biotech, UK) were added to a final activity of  $3 \text{ KBq ml}^{-1}$  in all the experiments. The specific activities were  $74.0 \text{ MBq ml}^{-1}$  for calcium,  $2.0 \text{ GBq mmol}^{-1}$  for bicarbonate and  $12.0 \text{ GBq mmol}^{-1}$  for glucose.

Two experimental conditions were applied; the first was illumination with  $170\text{-}\mu\text{mol photons m}^{-2} \text{s}^{-1}$ , and the second was dark incubations. Controls for isotopic exchange were done with killed specimens by 2% formaldehyde.

### Processing of the samples after incubation

After the incubation, the coral colonies were extensively washed in 2 l filtered seawater (two successive times, 5 min each). After washing, single polyps were separated from the mother colony by a wire cutter. The skeletons that were not covered with tissue were discarded. After that, the colonies and the polyps were heated in 2 N NaOH at 90°C for 20 min to hydrolyze the tissue. The skeletons were washed several times with NaOH solution to remove the tissue within the corallite. Decay per minute (dpm) in the hydrolysate was determined using a Packard TR 2500 scintillation counter operating in efficiency tracing mode to correct for quench. The skeletons were then washed with distilled water to remove nonspecifically bound tracer and dried at 50°C overnight. The next day, the skeletons incubated in  $^{45}\text{Ca}$  were weighed and hydrolyzed in 12 N HCl solution and the activity was counted.  $\text{CO}_2$ -trapping (for the colonies labeled with  $^{14}\text{C}$ ) was done according to the method of Boetius et al. (2001) with slight modification after T. Treude (in preparation).

In another set of experiments, skeletons from the previous experiments were immersed in epoxy resin for  $\beta$ -Imaging. After 2 days in the resin, a diamond rock saw (CONRAD D 33892 CLAUSTHAL-ZELLERFELD rock saw) was used to make 2 mm thick longitudinal slices of the corallites.

### $\beta$ -Imaging

Autoradiography of the coral slices were acquired in 12 h exposure (fixed time for all the samples) in a Micro-Imager described in Laniece et al. (1998). Briefly, the Micro-Imager is a new technology that allows quantitative real time analysis of radiolabelled samples with a high spatial resolution and high detection sensitivity. In this machine, the light generated by the ionizing radiation ( $\alpha$ ,  $\beta$ ,  $\gamma$ ) in a thin solid scintillator is amplified by an

image intensifier, consisting of a few million 10  $\mu\text{m}$  quartz capillaries. The amplified light is then transmitted to a high resolution charge-coupled device (CCD) camera connected to a PC equipped with software for the analysis of such data. The sensitive area is 2.4 cm  $\times$  3.2 cm and the measuring time depends on the radioactivity in the sample, ranging from minutes to hours. Each coral slice was positioned on a microscopic slide and covered with a scintillating sheet. The device allows 10–15  $\mu\text{m}$  spatial resolution. As the micro-imager was used to quantify the local radioactivity intensity of  $\beta$ -emitters, we refer to the ensuing data as  $\beta$ -counts and  $\beta$ -images.

A digital camera was used to photograph the coral slices to be compared with the images developed by the Micro-Imager.

## Results

The Pg was very heterogeneously distributed over a single polyp. The rates of Pg were found highest on the top parts of the *G. fascicularis* polyp (Fig. 2). The tissue covering the base of the septum and the middle piece of the tentacles had rates of  $0.041 \pm 0.003$  ( $n=5$ ) moles  $\text{O}_2 \text{ m}^{-3} \text{ s}^{-1}$  and  $0.035 \pm 0.003$  ( $n=5$ ) moles  $\text{O}_2 \text{ m}^{-3} \text{ s}^{-1}$ , respectively. However, the very tips of the septa had a very low Pg rate. The mouth and adjacent tissue had Pg rates ranging from  $0.0245 \pm 0.002$  to  $0.029 \pm 0.003$  ( $n=5$ ) (ca. 60–70% of the rates on the septum and the tentacle). Pg in the tissue covering the wall of the polyp was 10% of that of the septum and tentacle. The lowest Pg rate was found on the coenosarc (the tissue connecting adjacent polyps).

Also  $^{45}\text{Ca}$  incorporation was very heterogeneous. The coral corallites septa incorporated more  $^{45}\text{Ca}$  than the bottom parts in both light and dark as indicated by the  $\beta$ -images and the  $\beta$ -counts of the slices (Fig. 3). The light incubated colonies had a ca. 58% higher  $^{45}\text{Ca}$  incorporation rate in its skeletons compared to the dark incubated ones (Fig. 4). The rate of calcification is  $0.964 \pm 0.28$  ( $n=4$ )  $\mu\text{mol Ca}^{2+} \text{ g}^{-1}$  skeleton weight  $\text{h}^{-1}$

in light and  $0.612 \pm 0.11$  ( $n=4$ )  $\mu\text{mol Ca}^{2+} \text{ g}^{-1}$  skeleton weight  $\text{h}^{-1}$  in dark (Student *T*-test,  $P=0.021$ ).

Skeletons of the dead colonies incorporated 4–6% of the tracer relative to the living colonies. Only a background activity image was obtained upon imaging of the corallite slices of the dead colonies (Fig. 3).

The tissue fraction had very little  $^{45}\text{Ca}$  incorporation in both light and dark conditions. The rate of incorporation is ca.  $0.016 \pm 0.002$  ( $n=4$ )  $\mu\text{mol Ca}^{2+} \mu\text{g}^{-1}$  protein  $\text{h}^{-1}$  and ca.  $0.016 \pm 0.0004$  ( $n=4$ )  $\mu\text{mol Ca}^{2+} \mu\text{g}^{-1}$  protein  $\text{h}^{-1}$  in light and dark incubations, respectively ( $P=0.292$ ). About 85% (ca.  $0.014 \pm 0.002$  ( $n=4$ )  $\mu\text{mol Ca}^{2+} \mu\text{g}^{-1}$  protein  $\text{h}^{-1}$ ) relative to the tissue fractions of the living colonies was found in the tissue fraction of the dead colonies (Fig. 4).

Heterogeneity was also observed when the coral colonies were incubated in  $^{14}\text{C-HCO}_3^-$  (Fig. 5). The  $\beta$ -images of the corallites slices and  $\beta$ -counts revealed that the septa incorporated most of the radioactive tracer. The corallites incorporated the tracer ca. 67% higher in light compared to dark (Fig. 6a). The rate of calcification depending on  $^{14}\text{C-HCO}_3^-$  incorporation is ca.  $1.03 \pm 0.09$  ( $n=4$ )  $\mu\text{mol HCO}_3^- \text{ g}^{-1}$  skeleton weight  $\text{h}^{-1}$  and ca.  $0.61 \pm 0.09$  ( $n=4$ )  $\mu\text{mol HCO}_3^- \text{ g}^{-1}$  skeleton weight  $\text{h}^{-1}$  in light and dark, respectively ( $P=0.001$ ). Only 2.5 and 4.1% of the tracer relative to the living colonies incubated in light and dark, respectively, was incorporated in the corallites of the formaldehyde treated colonies. The  $\beta$ -image of this treatment showed only a background activity in the corallite slice (Fig. 5).

The  $^{14}\text{C-HCO}_3^-$  tracer incorporation in tissue fraction is ca. 10 times higher in light than in dark (Fig. 6a). The rate of tracer incorporation is ca.  $0.16 \pm 0.0067$  ( $n=4$ )  $\mu\text{mol HCO}_3^- \mu\text{g}^{-1}$  protein  $\text{h}^{-1}$  and  $0.016 \pm 0.006$  ( $n=4$ )  $\mu\text{mol HCO}_3^- \mu\text{g}^{-1}$  protein  $\text{h}^{-1}$  in light and dark, respectively ( $P=8.8 \times 10^{-8}$ ). The tissue fraction of the dead colonies had ca. 2.8 and 27% tracer incorporation, relative to the living colonies incubated in light and dark, respectively.

The total  $^{14}\text{C-HCO}_3^-$  tracer incorporation in the skeleton and tissue fractions is about 4 $\times$  higher in light than in dark (Fig. 6b). In light, ca. 32% of the total tracer incorporation was found in the skeleton and ca. 68% in the tissue. In dark, ca. 75% of the tracer was found in the skeleton fraction and only 25% in the tissue fraction.

Incubation with  $^{14}\text{C}$ -labelled glucose showed similar trend in the radioactive tracer incorporation in the corallites with the top parts being more active in the tracer incorporation in light and dark conditions (Fig. 7). The corallites were more active in the tracer incorporation in light than in dark. The dark incubated colonies incorporated ca. 58% of the tracer in their skeletons relative to the light incubated colonies ( $P=0.018$ ) (Fig. 8A). The dead colonies incubated in the presence of 2% formaldehyde did not incorporate the tracer in their skeletons and only a background image was observed upon imaging (Fig. 7). Only 0.6 and 1.1% tracer incorporation relative to the light and dark

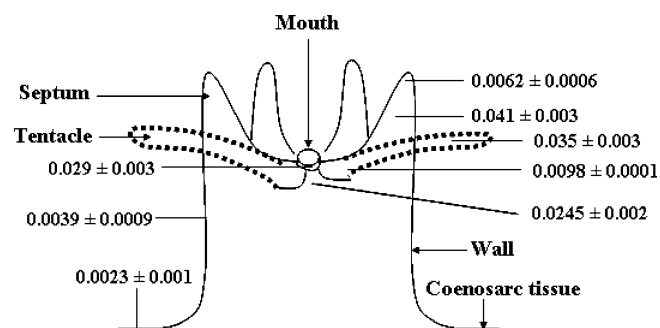
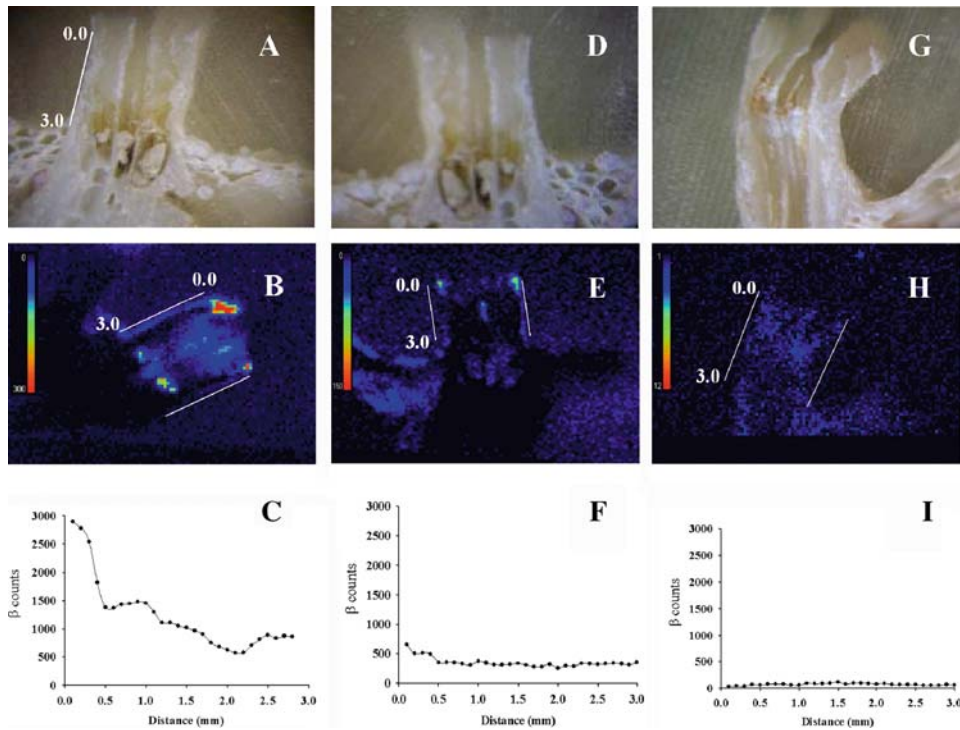


Fig. 2 Schematic drawing of a *G. fascicularis* polyp showing the rates of Pg measured at the sites specified. The rates are expressed in mole  $\text{O}_2 \text{ m}^{-3} \text{ s}^{-1}$



**Fig. 3** Results from the Micro-Imager for the *G. fascicularis* colonies incubated with  $^{45}\text{Ca}$ . **a** Digital photo of a longitudinal slice of corallite after incubation in light. **b**  $\beta$ -Image of the slice in **a**. **c**  $\beta$ -Count of the image in **b** along the transect between the *two white lines*. **d** Digital photo of a longitudinal slice of corallite after incubation in dark. **e**  $\beta$ -Image of the slice in **d**. **f**  $\beta$ -Count of the image in **e** along the transect between the *two white lines*. **g** Digital photo of a longitudinal slice of corallite killed with 2% formaldehyde. **h**  $\beta$ -Image of the slice in **g**. **i**  $\beta$ -Count of the image in **h** along the transect between the *two white lines*. The  $\beta$ -Counts (**c**, **f**, **i**) were done for the cross sectional area over distance between the *two vertical lines* in the corresponding images (**b**, **e**, **h**). The colors in **b**, **e** and **h** represent the intensity of the radio-activity in the images, quantified according to the *color scale on the left*. For the transects the pixel intensities between the *two white lines* were averaged

incorporation rates in both light and dark conditions were obtained (Fig. 8a). The rate is ca.  $2.28 \pm 0.33$  ( $n=4$ )  $\text{nmol glucose } \mu\text{g}^{-1} \text{ protein h}^{-1}$  and ca.  $2.34 \pm 0.23$  ( $n=4$ )  $\text{nmol glucose } \mu\text{g}^{-1} \text{ protein h}^{-1}$  in light and dark, respectively ( $P=0.79$ ). The dead colonies incubated in 2% formaldehyde incorporated only 0.5% of the tracer in their tissue fractions relative to the living colonies.

Coral tissue incorporated  $^{14}\text{C}$  from glucose more actively than the skeleton. In both light and dark conditions, 6% of the radioactive tracer was found in the skeleton fraction, while 94% was found in the tissue fraction (Fig. 8b). The total  $^{14}\text{C}$ -glucose incorporation in the two fractions was ca. 40% higher in light than in dark.

incubated colonies, respectively were found in the skeletons of the dead colonies (Fig. 8a).

Illumination had little effect on the rates of  $^{14}\text{C}$ -glucose incorporation in the coral tissue and similar

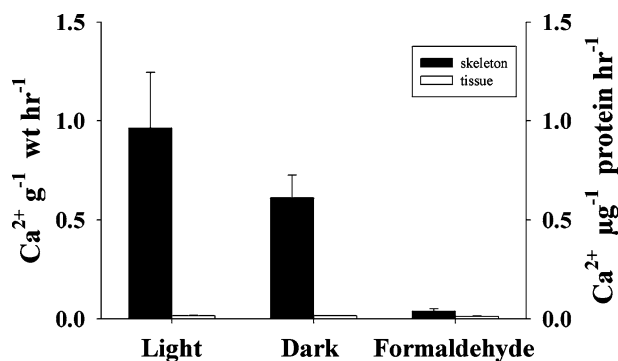


**Fig. 4**  $^{45}\text{Ca}$  incorporation in the skeleton and the tissue fractions of *G. fascicularis* after incubation in light, dark and in the presence of 2% formaldehyde. The y-axis to the left is for skeleton values and one to the right is for tissue values. Bars represent mean  $\pm$  SD

## Discussion

Oxygen production in *G. fascicularis* was found to be highly heterogeneous on the surface of their polyps (Fig. 2). The rate of Pg was found highest on the tissue covering the middle parts of the corallite septa, the tentacles, and the tissue surrounding the mouth of the polyp. The tissues covering the white tips of the septa, the wall of the polyp and the coenosarc (the tissue that connects polyps in the colony) had ca. 1 order of magnitudes lower Pg rates.

The main product of photosynthesis is the reduced organic carbon compounds. In corals, most of the organic carbon compounds produced by the zooxanthellae are transported to the animal (Muscatine et al. 1981, 1984). This can be used as an energy reservoir as well as building blocks during biosynthesis in the polyp. On the other hand, the oxygen produced during photosynthesis

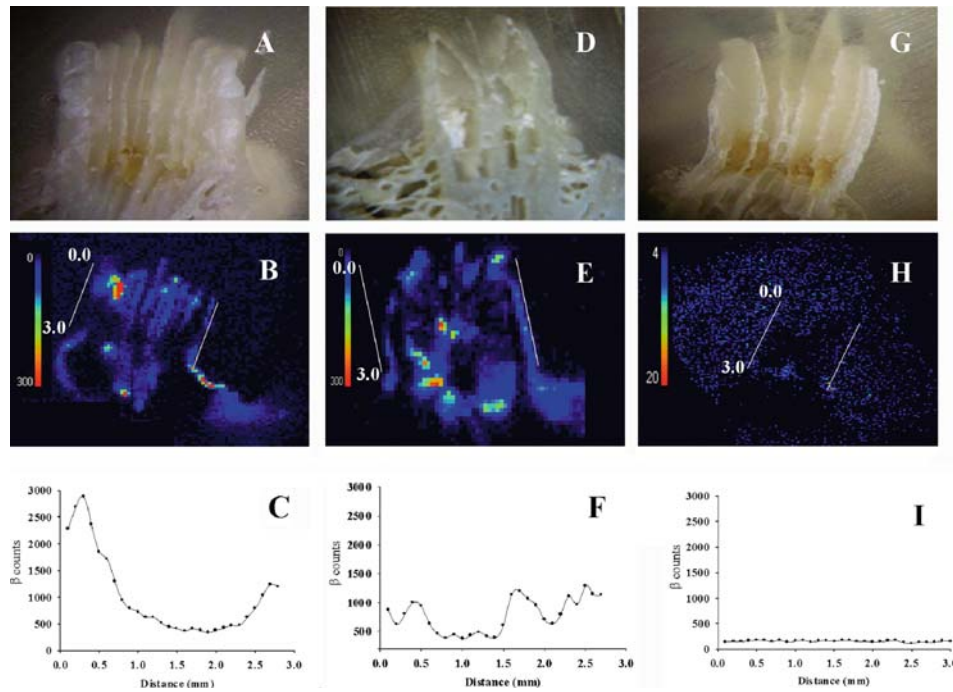


**Fig. 5** Results from the Micro-Imager for the *G. fascicularis* colonies incubated with  $^{14}\text{C-HCO}_3^-$ . **a** Digital photo of a longitudinal slice of corallite after incubation in light. **b**  $\beta$ -Image of the slice in **a**. **c**  $\beta$ -Count of the image in **b** along the transect between the two white lines. **d** Digital photo of a longitudinal slice of corallite after incubation in dark. **e**  $\beta$ -Image of the slice in **d**. **f**  $\beta$ -Count of the image in **e** along the transect between the two white lines. **g** Digital photo of a longitudinal slice of corallite killed with 2% formaldehyde. **h**  $\beta$ -Image of the slice in **g**. **i**  $\beta$ -Count of the image in **h** along the transect between the two white lines. The  $\beta$ -counts (**c**, **f**, **i**) were done for the cross sectional area over distance between the two vertical lines in the corresponding images (**b**, **e**, **h**). The colors in **b**, **e**, and **h** represent the intensity of the radio-activity in the images, quantified according to the color scale on the left. For the transects the pixel intensities between the two white lines were averaged

helps in maintaining an oxic condition in the coral. Both products, reduced carbon compounds and oxygen, are used in production of ATP, which is required by calcification. Thus, the high rates of Pg in the top parts of the coral polyp indicate high rates of energy and organic carbon production in those polyp parts.

The rate of Pg in corals is dependant on the number and activity of zooxanthellae and the light field in the spot measured. The spatial distribution of zooxanthellae and the cell specific density (number of zooxanthellae per host cell) on the polyp surface is determined by the tissue architecture and the general colony morphology (Helmuth et al. 1997; Muscatine et al. 1998). The efficiency of light capturing is influenced by the polyp shape (Porter 1976). It was found by Kühl et al. (1995) that the light field at the tissue surface of the coral differs strongly with respect to intensity and spectral composition. Thus, the zooxanthellae productivity differs in the different localities on the coral surface as it is reflected by the heterogeneous distribution of Pg rates. This in turn will strongly affect the coral metabolism in the vicinity of

the adjacent polyp parts. The more the energy and organic carbon produced, the higher can the growth rates be of the connected polyp parts.

When *G. fascicularis* colonies were incubated in the presence of  $^{45}\text{Ca}$ , the radioactive tracer incorporation

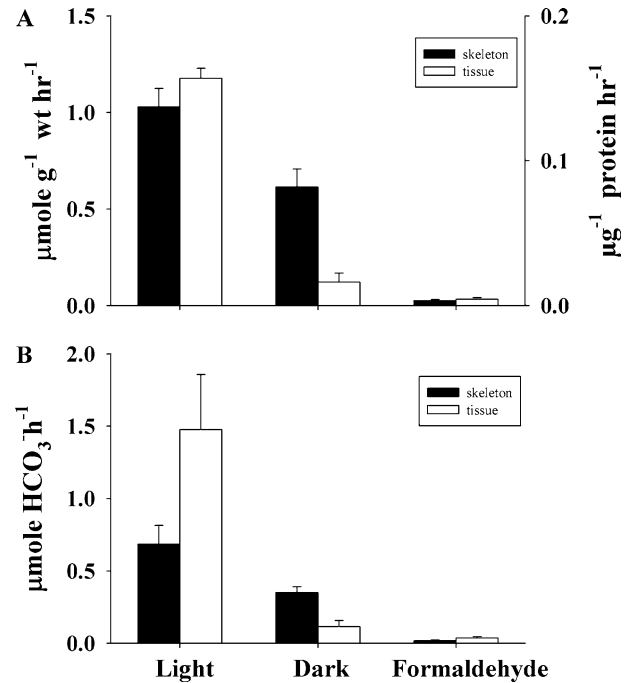


**Fig. 6** **a** Incorporation of  $^{14}\text{C}$  in the skeleton and tissue fractions of *G. fascicularis* incubated with  $^{14}\text{C-HCO}_3^-$  in light, dark and in the presence of 2% formaldehyde, the y-axis to the left is for skeleton values and one to the right is for tissue values. **b** Distribution of the total tracer incorporated between the skeleton and tissue fractions. Bars represent mean  $\pm$  SD

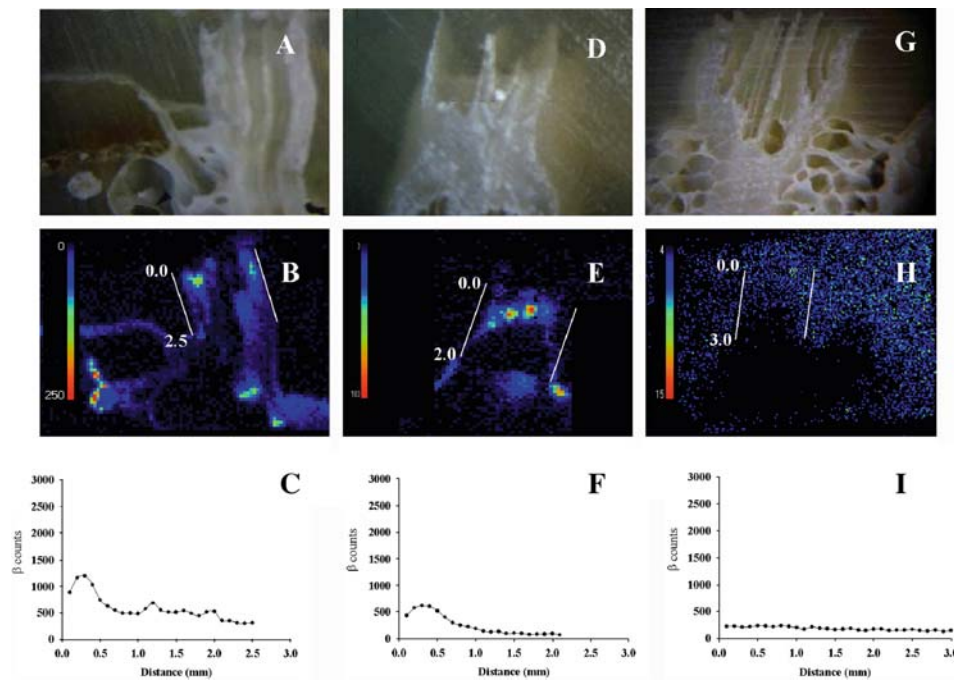


**Fig. 7** Results from the Micro Imager for the *G. fascicularis* colonies incubated with  $^{14}\text{C}$ -glucose. **a** Digital photo of a longitudinal slice of corallite after incubation in light. **b**  $\beta$ -Image of the slice in **a**. **c**  $\beta$ -Count of the image in **b** along the transect between the two white lines. **d** Digital photo of a longitudinal slice of corallite after incubation in dark. **e**  $\beta$ -Image of the slice in **d**. **f**  $\beta$ -Count of the image in **e** along the transect between the two white lines. **g** Digital photo of a longitudinal slice of corallite killed with 2% formaldehyde. **h**  $\beta$ -Image of the slice in **g**. **i**  $\beta$ -Count of the image in **h** along the transect between the two white lines. The  $\beta$ -counts (**c**, **f**, **i**) were done for the cross sectional area over distance between the two vertical lines in the corresponding images (**b**, **e**, **h**). The colors in **b**, **e**, and **h** represent the intensity of the radio-activity in the images, quantified according to the color scale on the left. For the transects the pixel intensities between the two white lines were averaged

into the coral corallites was not homogeneous (Fig. 3). The corallites incorporated more  $^{45}\text{Ca}$  in its highermost parts, specifically the tips of the septa, compared to the lower parts, the walls and the coenosteum (the skeletal material between the corallites). The  $\beta$ -count of the corallite image in light showed a steep decrease in the activity from top to bottom of the  $\beta$ -image (Fig. 3). This indicates differences in calcification rates among those parts of the polyp. The results are consistent with the findings of Marshall and Wright (1998) where they have shown that the  $^{45}\text{Ca}$  was incorporated differently in the cross sections of coral corallite. Both light incubated and dark incubated colonies showed a similar pattern of  $^{45}\text{Ca}$  incorporation, although the overall  $^{45}\text{Ca}$  incorporation is higher in light than in dark (Fig. 4). This suggests that the distribution pattern of calcification on the corallite surface is morphogenetically determined rather than being affected by the light field. Based on  $^{45}\text{Ca}$  uptake, the calcification rate in light is close to  $1 \mu\text{mol g}^{-1}$  skeleton weight  $\text{h}^{-1}$ , a rate that lies within the range reported for other scleractinian corals (Erez

1978). This rate is about 58% higher than dark calcification, which confirms previous observations in corals (e.g. Goreau 1959).

Calcification in corals was shown to be an energy demanding process (Chalker and Taylor 1975; Krishnaveni et al. 1989; Tambutte et al. 1996). Thus, the higher rates of calcification in the top parts of the polyp necessitate a higher rate of energy supply to those parts. The high energy demand for those parts is possibly supplied through the high rates of photosynthesis in the adjacent polyp parts. Although the very tips of the septa showed low rates of Pg, reduced organic carbon compounds produced by zooxanthellae in the lower tissues can be translocated to the growing tips where ATP can be generated for calcification (Pearse and Muscatine 1971; Fang et al. 1989).

Although the use of radioactive isotopes in studying coral calcification started some 50 years ago (Goreau 1959), estimation of isotopic exchange remained a problem (Tambutte et al. 1996). Error associated with isotopic exchange were reduced by using cultured microcolonies with no skeletons exposed to the radioisotope-labelled incubation medium (Tambutte et al. 1995), but it is still difficult to distinguish isotopic exchange from dark calcification (Chalker and Taylor 1975; Marshall and Wright 1998). To distinguish the difference between isotopic exchange and dark calcification, colonies were killed with 2% formaldehyde and incubated in a similar way to the living colonies. In this way, we could exclude all the biological factors without removing the tissue layer, which helps in forming a barrier for isotopic exchange (Goreau 1959). The results showed a large difference between the dark incubated colonies and the dead ones, with much higher tracer incorporation in the dark incubated

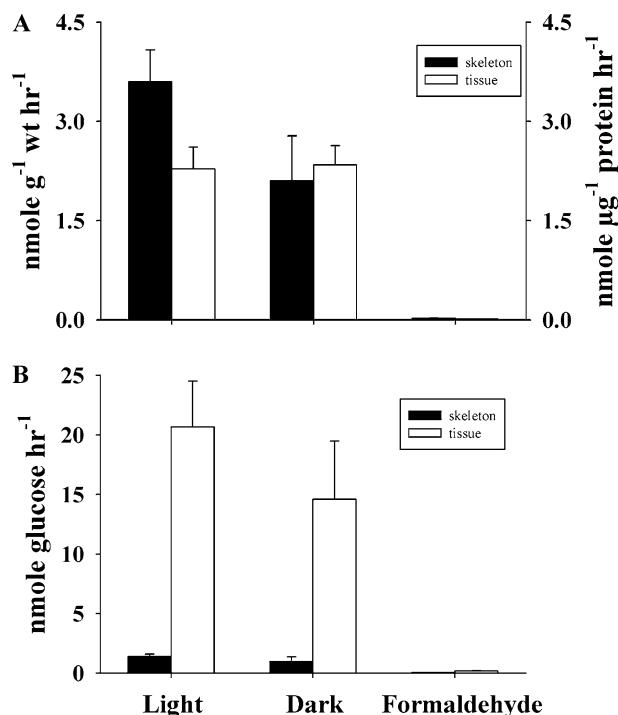


**Fig. 8** a Incorporation of  $^{14}\text{C}$  in the skeleton and tissue fractions of *G. fascicularis* incubated with  $^{14}\text{C}$ -glucose in light, dark and in the presence of 2% formaldehyde, the y-axis to the left is for skeleton values and the one to the right is for tissue values. b Distribution of the total tracer incorporated between the skeleton and tissue fractions. Bars represent mean  $\pm$  SD

colonies compared to the dead colonies. Thus, dark calcification does indeed exist and is not an artifact of isotopic exchange.

The tissue fraction did not incorporate  $^{45}\text{Ca}$  in both light and dark incubated colonies. The coral colonies incorporated ca.  $0.016 \mu\text{mol Ca}^{2+} \mu\text{g}^{-1} \text{protein h}^{-1}$  in their tissue fractions under both light and dark conditions (Fig. 4). This is similar to the amount of tracer found in the tissue fraction of the dead colonies, indicating that only physical diffusion of the tracer is responsible for it rather than the reason being incorporation into the tissue. With the radioactive tracer method, it is not possible to evaluate whether an active transport system exists in the tissue or not, the animal tissue maintains very low intracellular  $\text{Ca}^{2+}$  concentrations (Barnes and Chalker 1990). Other methods are required such as microsensors to demonstrate the presence of an active transport mechanism for  $\text{Ca}^{2+}$  ions (Al-Horani et al. 2003).

The incorporation pattern of  $^{14}\text{C}\text{-HCO}_3^-$  into the coral corallites was similar to that of  $^{45}\text{Ca}$  incorporation (Fig. 5). The corallite septa were more active in the tracer incorporation in both light and dark incubations. The ratio of light to dark incorporation of the  $^{14}\text{C}\text{-HCO}_3^-$  tracer was close to that of  $^{45}\text{Ca}$ . Based on  $^{14}\text{C}\text{-HCO}_3^-$  uptake, the rate of calcification is ca.  $1.03 \mu\text{mol HCO}_3^- \text{g}^{-1} \text{skeleton weight h}^{-1}$ , a value close to that calculated from  $^{45}\text{Ca}$  uptake. The rate in dark is the

same as that obtained with  $^{45}\text{Ca}$  uptake giving a stoichiometric ratio of 1:1 for calcium and carbon uptake in the coral  $\text{CaCO}_3$  skeleton. The dead colonies did not incorporate the  $^{14}\text{C}$  tracer into their skeletons confirming the results obtained with  $^{45}\text{Ca}$ .

A main difference between the  $^{14}\text{C}\text{-HCO}_3^-$  and  $^{45}\text{Ca}$  incorporation was observed in the tissue incorporation of the tracer. About 68% of the total incorporated  $^{14}\text{C}\text{-HCO}_3^-$  tracer in the whole colony was found in the tissue fraction in light (Fig. 6b). Under dark conditions, only 25% of the total incorporation of  $^{14}\text{C}\text{-HCO}_3^-$  tracer was found in the tissue fraction, while 75% was found in the skeleton fraction. Obviously, photosynthesis is the main process responsible for the  $\text{HCO}_3^-$  incorporation in the tissue in light. Active transport of  $\text{HCO}_3^-$  may be involved in the dark incorporation of the  $\text{HCO}_3^-$  (Furla et al. 2000). The total  $^{14}\text{C}\text{-HCO}_3^-$  incorporation in both tissue and skeleton increased four folds in light, which shows that no competition between photosynthesis and calcification for dissolved inorganic carbon exists.

In another set of experiments,  $^{14}\text{C}$ -labelled glucose was added to the incubation medium as an external energy and carbon source. Although glucose is normally present in low concentrations in the sea, the corals are efficient in using it as an energy source (Stephens 1960). The data showed that *G. fascicularis* incorporates the  $^{14}\text{C}$  tracer from glucose in its skeletons and tissues in both light and dark conditions. The pattern of incorporation into the corallite is similar to the incorporation of the  $^{45}\text{Ca}$  and  $^{14}\text{C}\text{-HCO}_3^-$  with the top part being more active in incorporating the tracer (Fig. 7).

In the corallites, the incorporation of  $^{14}\text{C}$  from glucose was higher in light than in dark. This could be attributed to the enhanced rates of coral calcification and respiration in light (Chalker and Taylor 1975; Kühl et al. 1995). Because the use of glucose is dependant on the respiration efficiency, the respiration in dark is limited by the diffusive supply of oxygen through the diffusive boundary layer (Kühl et al. 1995), while in light, photosynthesis creates oxic environment in the coral, thereby enhancing respiration. The incorporation of  $^{14}\text{C}$  from  $\text{HCO}_3^-$  and glucose into the coral skeleton is consistent with the hypothesis that both carbon sources are used in coral calcification (Goreau 1977; Erez 1978).

Unlike the incorporation of  $^{45}\text{Ca}$  and  $^{14}\text{C}\text{-HCO}_3^-$ , most of the  $^{14}\text{C}$ -glucose incorporated in the coral was found in the tissue fraction in both light and dark conditions (Fig. 8b). In both light and dark conditions, about 94% of the total incorporated  $^{14}\text{C}$ -glucose tracer was found in the tissue fraction, while only 6% was found in the skeleton fraction. Glucose incorporation into the tissue was not affected by the light condition, showing that it is not a light dependant process.

There was no isotopic exchange in the case of  $^{14}\text{C}$ -glucose incubation in both skeleton and tissue fractions in light and dark incubations. The very small amount of the tracer (0.6–1.1% of the total incorporation relative to the living colonies) found in the tissue and skeleton of the dead colonies can be attributed to nonspecific

binding. In the case of  $^{14}\text{C-HCO}_3^-$ , 2.5 and 4.1% of the tracer incorporation in the skeleton in light and dark, respectively, is attributed to isotopic exchange. These values should be considered for the estimation of calcification rates in corals when using radioactive tracers.

The growth pattern of the coral corallites is a morphogenetically controlled process, while the growth rate is light dependant. The higher rates of skeletal growth are supported by higher rates of photosynthesis and respiration in the adjacent polyp parts.

**Acknowledgements** This study was funded by Max Planck Institute for Marine Microbiology-Bremen, Germany. We thank G. Eickert, A. Eggers and I. Schröder for constructing the oxygen electrodes, S. Rousan (from University of Bremen) and N. Finke, H. Jonkers (from the MPI-Bremen) for technical support. We also thank the staff of the Marine Science Station in Aqaba-Jordan for supplying the diving equipment, Laboratory space and coral specimens.

## References

- Al-Horani FA, Al-Moghrabi SM, de Beer D (2003) The mechanism of calcification and its relation to photosynthesis and respiration in the scleractinian coral *Galaxea fascicularis*. *Mar Biol* 142:419–426
- Allemand D, Furla P, Benazet-Tambutte S (1998) Mechanisms of carbon acquisition for endosymbiont photosynthesis in Anthozoa. *Can J Bot* 76:925–941
- Barnes DJ, Chalker BE (1990) Calcification and photosynthesis in reef-building corals and algae. In: Dubinsky Z (ed) *Coral reefs*. Elsevier, Amsterdam, pp 109–131
- Boetius A, Ferdelmann T, Lochte K (2001) Bacterial activity in sediments of the deep Arabian Sea in relation to vertical flux. *Deep-Sea Res II* 47:2835–2875
- Chalker BE, Taylor DL (1975) Light-enhanced calcification, and the role of oxidative phosphorylation in calcification of the coral *Acropora cervicornis*. *Proc R Soc Lond B* 190:323–331
- De Beer D, Kühl M, Stambler N, Vaki L (2000) A microsensor study of light enhanced  $\text{Ca}^{2+}$  uptake and photosynthesis in the reef-building hermatypic coral *Favia* sp. *Mar Ecol Prog Ser* 194:75–85
- Dubinsky Z, Stambler N, Ben-Zion M, McCloskey L, Muscatine L, Falkowski PG (1989) The effect of external nutrient resources on the optical properties and photosynthetic efficiency of *Stylophora pistillata*. *Proc R Soc Lond B* 239:231–246
- Erez J (1978) Vital effect on stable-isotope composition seen in foraminifera and coral skeletons. *Nature* 273:199–202
- Fang LS, Chen YWJ, Chen CS (1989) Why does the white tip of stony coral grow so fast without zooxanthellae?. *Mar Biol* 103:359–363
- Furla P, Benazet-Tambutte S, Allemand D, Jaubert J (1998) Diffusional permeability of dissolved inorganic carbon through the isolated oral epithelial layers of the sea anemone, *Anemonia viridis*. *J Exp Mar Biol Ecol* 221:71–88
- Furla P, Galgani I, Durand I, Allemand D (2000) sources and mechanisms of inorganic carbon transport for coral calcification and photosynthesis. *J Exp Biol* 203:3445–3457
- Gattuso JP, Allemand D, Frankignoulle M (1999) Photosynthesis and calcification at cellular, organismal and community levels in coral reefs: a review on interaction and control by carbonate chemistry. *Am Zool* 39:160–183
- Goreau TF (1959) The physiology of skeleton formation in corals. I. A method for measuring the rate of calcium deposition by corals under different conditions. *Biol Bull* 116:59–75
- Goreau TF (1963) Calcium carbonate deposition by coralline algae and corals in relation to their roles as reef-builders. *Ann N Y Acad Sci* 109:127–167
- Goreau TJ (1977) Coral skeletal chemistry: physiological and environmental regulation of stable isotopes and trace metals in *Montastrea annularis*. *Proc R Soc Lond B* 196:291–315
- Helmuth BST, Timmerman BEH, Sebens KP (1997) Interplay of host morphology and symbiont microhabitat in coral aggregation. *Mar Biol* 130:1–10
- Kühl M, Cohen Y, Dalsgaard T, Jorgensen BB, Revsbech NP (1995) Microenvironment and photosynthesis of zooxanthellae in scleractinian corals studied with microsensors for  $\text{O}_2$ , pH and light. *Mar Ecol Prog Ser* 117:159–172
- Krishnaveni P, Chou LM, Ip YK (1989) Deposition of calcium ( $^{45}\text{Ca}$ ) in the coral, *Galaxea fascicularis*. *Comp Biochem Physiol* 94A:509–513
- Laniece P, Charon Y, Cardona A, Pinot L, Maitrejean S, Mastroianni R, Sandkamp B, Valentin L (1998) A new high resolution radioimager for the quantitative analysis of radiolabelled molecules in tissue section. *J Neurosci Methods* 86:1–5
- Marshall AT, Wright A (1998) Coral calcification: autoradiography of a scleractinian coral *Galaxea fascicularis* after incubation in  $^{45}\text{Ca}$  and  $^{14}\text{C}$ . *Coral Reefs* 17:37–47
- Muscatine L, McCloskey LR, Marian RE (1981) Estimating the daily contribution of carbon from zooxanthellae to coral animal respiration. *Limnol Oceanogr* 26(4):601–611
- Muscatine L, Falkowski PG, Porter JW, Dubinsky Z (1984) Fate of photosynthetic fixed carbon in light- and shade-adapted colonies of the symbiotic coral, *Stylophora pistillata*. *Proc R Soc Lond B* 222:181–202
- Muscatine L, Ferrier-Pages C, Blackburn A, Gates RD, Baghdarian G, Allemand D (1998) Cell-specific density of symbiotic dinoflagellates in tropical Anthozoans. *Coral Reefs* 17:329–337
- Pearse VB, Muscatine L (1971) Role of symbiotic algae (zooxanthellae) in coral calcification. *Biol Bull* 141:350–363
- Porter JW (1976) Autotrophy, heterotrophy, and resource partitioning in Caribbean reef building corals. *Am Nat* 110:731–742
- Revsbech NP, Jorgensen BB (1983) Photosynthesis of benthic microflora measured with high spatial resolution by the oxygen microprofile method. *Limnol Oceanogr* 28:749–756
- Simkiss K, Wilbur KM (1989) *Biomining: cell biology and mineral deposition*. Academic, UK
- Stephens GC (1960) Uptake of glucose from solution by solitary coral, *Fungia*. *Science* 131:1532
- Tambutte E, Allemand D, Bourge I, Gattuso JP, Jaubert J (1995) An improved  $^{45}\text{Ca}$  protocol for investigating physiological mechanisms in coral calcification. *Mar Biol* 122:453–459
- Tambutte E, Allemand D, Mueller E, Jaubert J (1996) A compartmental approach to the mechanisms of calcification in hermatypic corals. *J Exp Biol* 199:1029–1041